ISSN 1070-3632, Russian Journal of General Chemistry, 2011, Vol. 81, No. 5, pp. 978–985. © Pleiades Publishing, Ltd., 2011.
Original Russian Text © B.V. Shchetanov, Yu.A. Ivakhnenko, V.G. Babashov, 2010, published in Rossiiskii Khimicheskii Zhurnal, 2010, Vol. 54, No. 1, pp. 12–19.

Heat Shield Materials

B. V. Shchetanov, Yu. A. Ivakhnenko, and V. G. Babashov

All-Russian Scientific Research Institute of Aviation Materials Federal State Unitary Enterprise, State Research Center of the Russian Federation (RIAM), ul. Radio 17, Moscow, 105005 Russia
phone/fax: (499)2676177

Received December 1, 2009

Abstract—Some properties and applications in the aerospace industry of high-temperature whiskers (SiC, Si_3N_4, AlN) and fibers (SiO_2, $A1_2O_3$) are described.

DOI: 10.1134/S1070363211050288

The present paper focuses on the reusable outer plate heat shield coating (HSC). The most illustrative example of the application of plate heat shield coating is the heat shield of the Buran space shuttle (USSR) [1] and systems of the Space Shuttle family (USA) [2]. For other heat shield systems, see [3].

Plate Fiber Heat Shielding

The key constructive unit of a heat shield plate is a heat shield element (HSE) which consists of a fiber heat shield plate, erosion-resistant and lacquer coatings, a damping layer, and an adhesive joining the damping layer and plate, as well as the HSE as a whole and the space vehicle (SV) body (Fig. 1) [2].

Each material in this construction fulfills its special function, and in the absence of any of them the HSE as a whole, i.e. SV plate heat shield, will not work. Clearly, the key role here belongs to heat shield plates. These plates are fabricated of a fiber heat shield material (HSM) and constitute a rigid 3D matrix of inorganic high-temperature fibers fused together in their contact points by a special binder.

A principal question arises here: What fibers are necessary for plate HSM to be efficient and reliable? Therewith, it is important to note that the properties of an HSM (thermal conductivity, density, strength, thermal stability, thermal expansion coefficient) are primarily dependent on the fibers, i.e. on their composition, structure, morphology, etc., which are directly related to the fiber production technology. Clearly, strong as fibers may be, they should be fused with each other to form a strong bond at their contact sites. This is the second necessary condition for the production of a heat shield material meeting strength requirements.

Heat Shield Materials

Before dwelling on the types of heat shield materials, we would like to note the HSMs and whole heat shield systems of the Buran and Space Shuttle do not differ radically in construction, but the used materials are quite different [2].

The heat shield material of the Space Shuttle is based on silica fibers which are insufficiently thermally stable due to a high porosity. Moreover, these fibers contain oxide admixtures which, too,

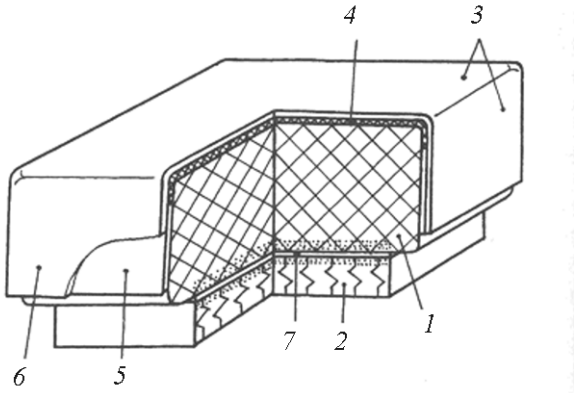

Fig. 1. Construction of a heat shield element: (*1*) plate of a fibrous heat shield material; (*2*) damping layer; (*3, 6*) lacquer moisture-proof coating; (*4, 5*) external and lateral erosion resistant coating; and (*7*) adhesive layer [2].

Table 1. Principal characteristics of fibers and whickers

Characteristic	Fibers		Whickers	
	$A1_2O_3$	Quartz (SiO_2)	Si_3N_4	SiC
X-ray composition	polycrystalline	amorphous	monocrystalline	monocrystalline
Diameter, μm	<3	1–2	1–5	<1
Density, g cm^{-3}	3.3–3.5	2.2	3.5–4.0	3
Working temperature, °C	1650	1250	1400	1400
Tensile strength, MPa	1000	<1000	10000	10000
Elasic modulus, GPa	150	80	300–400	570
Linear thermal expansion coefficient (LTEC), 10^{-6} deg^1	6.0–9.0	0.5	2.5–3.0	3.0–3.5
Linear shrinkage of fiber mat (without binder) over 14 h, %, no more than:				
at 1250°C	0	15	–	–
at 1600°C	2	–	–	–

adversely affect their thermal stability and favor crystallization of amorphous SiO_2 into α-crystoballite having an extremely high thermal expansion coefficient (TEC) in the temperature range 950–1100°C.

Consequently, the Li-900 and Li-2200 materials for the Space Shuttle [4], as well as the FRCI [5] and HTP materials [6] on the basis of silica fibers had, in our opinion, evidently insufficient thermal stability. Thus, the linear shrinkage of Li-900 after 16 h at 1250°C under isothermal heating conditions reached 25%.

This did not allow, when the need had arisen in improving radically the quality of plates, to be limited to modifying the silica system by active low-melting additives on the basis of B_2O_3. This would result in further enhancement of shrinkages and in-flight instability of plate geometry and size. The problem was solved by the development of principally new materials FRCI and then HTP, based on mixtures of SiO_2 fibers with higher melting $A1_2O_3$ fibers, such as Nextel (USA) and Saffil (Great Britain).

At our country, a fiborous heat shield material for plates was developed concurrently along several directions:

– from needle-like crystals (whiskers) of silicon carbide and nitride (VTNK material);

– from quartz fibers (TZMK series materials);

– from polycrystalline fibers (PCF) on the basis of alumina (TZMK-1700 material).

The principal characteristics of fibers and whiskers are listed in Table 1.

Whiskers of High-Melting Compounds

In terms of application in heat shield materials for flight vehicles, whiskers of high-melting compounds, specifically silicon carbide and nitride, offer the following advantages over other materials (aluminum oxide and nitride whiskers, aluminum oxide PCF, etc.):

– stable dimensions and phase composition, due to the monocrystallinity of the fibers;

– weak dependence of thermal conductivity on temperature, due to high radiation coefficients of silicon nitride and carbide;

– fairly low TEC (~$3–5\times10^{-6}$ deg^{-1}), close to graphite and intermediate between glass and oxides.

The drawbacks of these crystals relate to their oxidative instability and presence of non-fibrous inclusions in the bulk, which necessitates additional expenses for purification and increases the cost of already costly fibers. These drawbacks result from the very production technology of whiskers, involving gas-phase deposition.

The gas-phase deposition technique is based on condensation of whiskers from the gas–vapor phase containing vapors of crystal-forming elements or their gaseous (at the growth temperature) compounds. The target compound is formed by chemical reactions in

the vapor–gas phase and deposited, i.e. whisker formation involves the same processes and reactions as with epitaxial films, coatings, and powders.

Thus, silicon carbide whiskers are obtained via the following reaction sequence:

pyrolysis of methylsilanes

$$CH_3SiCl_3 \rightarrow SiC_{(s)} + 3HCl_{(g)},$$

substitution reaction between silicon tetrachloride and a hydrocarbon

$$SiCl_{4(g)} + CH_{4(g)} \rightarrow SiC_{(s)} + 4HCl_{(g)};$$

reaction with intermediate formation of volatile compounds, for example, SiO, which function as carriers in the gas phase:

$$SiO_{2(s)} + C_{(s)} \rightarrow SiO_{(g)} + CO,$$

$$SiO_{(g)} + CH_{4(g)} \rightarrow SiC + H_2O + H_2,$$

$$SiO_{2(s)} + C_{(s)} + CH_{4(g)} \rightarrow SiC_{(s)} + CO + H_2O + H_2.$$

The reaction sequence forming silicon nitride whiskers is as follows:

$$SiO_{2(s)} + Si_{(ж)} \rightarrow 2SiO_{(g)},$$

$$SiO_{(g)} + CO_{(g)} \rightarrow Si_{(g)} + CO_2,$$

$$CO_2 + C_s \rightarrow 2CO,$$

$$3Si_{(g)} + 2N_2 \rightarrow Si_3N_{4(s)}.$$

It was found that limiting in this sequence is the CO regeneration reaction. The necessary condition for this reaction is the presence in the growth zone of an open carbon surface. However, growth on a support is a low-performance process. On the other hand, melt crystallization which is sometimes used, is a still intricate and costly technique whose application is limited to a narrow range of oxygen-containing compounds.

Ii should be noted in the conclusion of this section that the mechanism of growth of such unusually shaped monocrystals as needle-like has been studied both by foreign and Russian researchers [7–12], since the growth process presents not only scientific but also and primarily practical interest.

In mid-1950s Sears suggested a diffusion dislocation model of whisker growth [7]. According to this model, the growth of whiskers, including those of refinery compounds, is made possible by the ingress on the support surface of screw dislocations which form a non-overgrown (like spiral stairs). However, this mechanism has not found practical application.

A different mechanism named "vapor–liquid–solid phase" (VLS) was suggested by Wagner and Ellis in mid-1960s [8, 9]. The principal idea of this theory consists in that the condensation on crystal growth occurs via an intermediate liquid phase rather than directly from the vapor to solid phase. The necessary and indispensable condition for whiskers to grow by this mechanism is the presence on the support of liquid droplets.

Our research [10–12] showed that whiskers can be grown if the growth zone is doped with solvent elements capable of forming liquid ternary solutions with the elements of the compound to be deposited, and then the latter is isolated by crystallization from the solution. Crystals grow by a more complicated mechanism which can be subdivided by the condensation and crystallization mechanisms. Therewith, condensation occurs by the VLT mechanism, whereas crystallization, both by the dislocation mechanism and the classical two-dimensional nucleation mechanism. Thus, in view of the known mechanism of whisker growth, the problem of developing an efficient continuous whisker production process restricted to the design and fabrication of the corresponding equipment.

In [11] we described in detail the methods for the production of whiskers and discussed different mechanisms of their production. The processes for the production of whiskers of such high-melting compounds as Al_2O_3, ZnO, AlN, SiC, and Si_3N_4 were commercialized. It should again be noted that the whisker growth process involves introduction of solvent elements, and, while present in small amounts, they still are undesirable admixtures in fibrous heat shield materials.

Unfortunately, silicon carbide and nitride, as already mentioned above, are prone to oxidation, which, in view of the high porosity and developed surface of fibrous materials, calls for extreme caution and very careful experimental testing to find out whether they are feasible for application in heat shield elements of flight vehicles. Due to a low thermal conductivity and a high air permeability of the material, heat released even upon slow oxidation can induce its spontaneous heating and thermal explosion, which may entail melting of the inner part of the plate. The situation is made still more complicated by the fact that, according to thermodynamic calculations and our experiments, under reduced atmospheric pressure, the SiC and Si_3N_4 oxidation reactions shift to form a

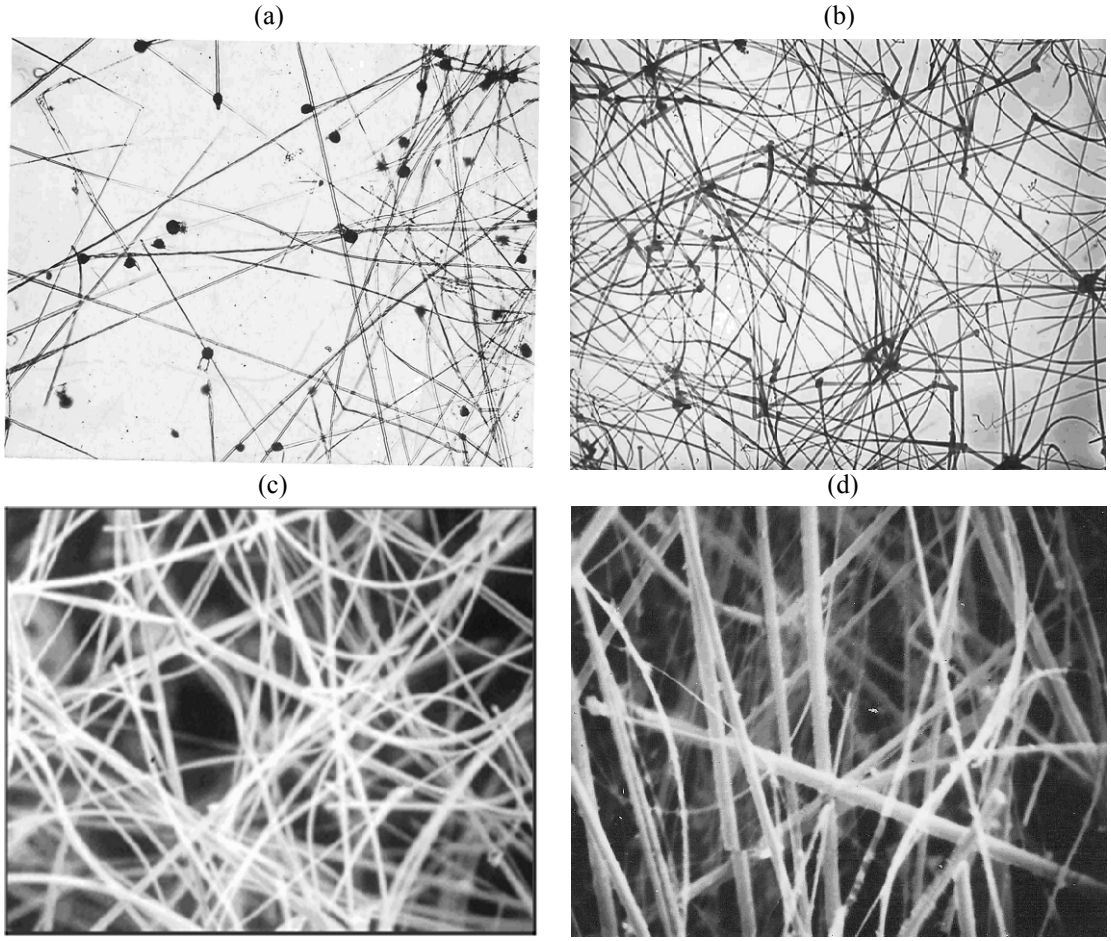

Fig. 2. (a, b) Whiskers and (c, d) fibers: (a) Si_3N_4, (b) SiC; (c) Al_2O_3; and (d) quartz (SiO_2).

gaseous SiO instead of a solid SiO_2, and, therefore, the SiO_2 film which commonly functions as the protective barrier disappears, and the oxidation rate, compared with that at atmospheric pressure, sharply increases. Production of SiC and Si_3N_4 whiskers was organized at the RIAM, but they have not found wide practical application. Figure 2 shows the micrographs of SiC and Si_3N_4 whiskers.

Fibers of High-Melting Compounds

Polycrystalline alumina fibers were chosen for fabrication of a heat shield plate due to their high thermal stability. The fibers were fabricated by the zol–gel procedure. The thermal stability and strength of fiber depends on whether it contains defects, primarily pores and structure imperfections. Pores arise by the following main reasons: insufficient degassing of the molding solution (MS); reaction of the MS with engineering equipment during fiber molding; evolution of volatiles during annealing of wet fibers; solid-phase reactions and phase transformations during annealing, which are accompanied by volume changes.

In a well-developed technology, the first two reasons are minimized, and we will not dwell on them here. As to the latter two reasons, a thermogravimetric study of the starting materials and fibers showed that all processes involving gas evolution largely occur below 300°C and are complete at 600°C, and the amorphous–crystal transition is complete about 800°C. A measure of open porosity is specific surface area which was determined by the BET nitrogen absorption method [13]. Therewith, the heating rate was the same as in the DTA and DTG study, namely100°C/h, with specific surface area measurements every 100°C. The objects for study were 3-μm 80 wt % Al_2O_3/20 wt % SiO_2 (80/20), as well as 90/10, and 72/28 (mullite stoichiometry) fibers.

Table 2. Volume fractions of mullite and α-Al_2O_3 at varied SiO_2 contents

Phase	SiO_2 content in the fiber, wt %				
	5	10	15	20	28
Mullite, vol %	20	38	56	74	100
α-Al_2O_3, vol %	80	63	44	26	0

Table 3. Linear shrinkages and dispersive strengths at varied SiO_2 contents

SiO_2 content in the fiber, wt %	l/d[a]	Linear shrinkage after annealing at 1700 °C, 8 h	Phase composition
5	80	8.2	α + mullite
10	100	8.2	α + mullite
20	100	3.6	α + mullite
28	150	20.0	mullite

[a] (l/d) Dispersive strength (measured after fiber annealing and dispersing), (l) fiber length, and (d) fiber diameter.

The temperature curves of fiber specific surface are show two peaks: at 400 and 900°C. The first peak is much lower that the second and disappears almost completely at ~600°C for all fibers, and the second peak does not disappear even at 1200°C. Thus, even though thermal treatment removes the most part of pores, their minor part still remains up to high temperatures [14].

Crystal Structure of Thermally Stable Fibers

Let us now turn to the crystal structure of thermally stable fibers. Obviously, it should remain sufficiently fine even after long-term exposure to high temperature. This can be provided by forming a finely disperse uniformly distributed two-phase structure, where stable phase grains prevent indefinite growth of each other. In our case, these are mullite ($3Al_2O_3{\cdot}2SiO_2$) and α-Al_2O_3.

Structural study of fibers showed that a colloidal SiO_2 particle (particle size ~10–30 nm) preserves its morphology up to 1250°C until it passes into mullite which inherits this morphology, but the particle diameter increases ~ in 1.5 times. This fact established by direct observations at an electron microscope

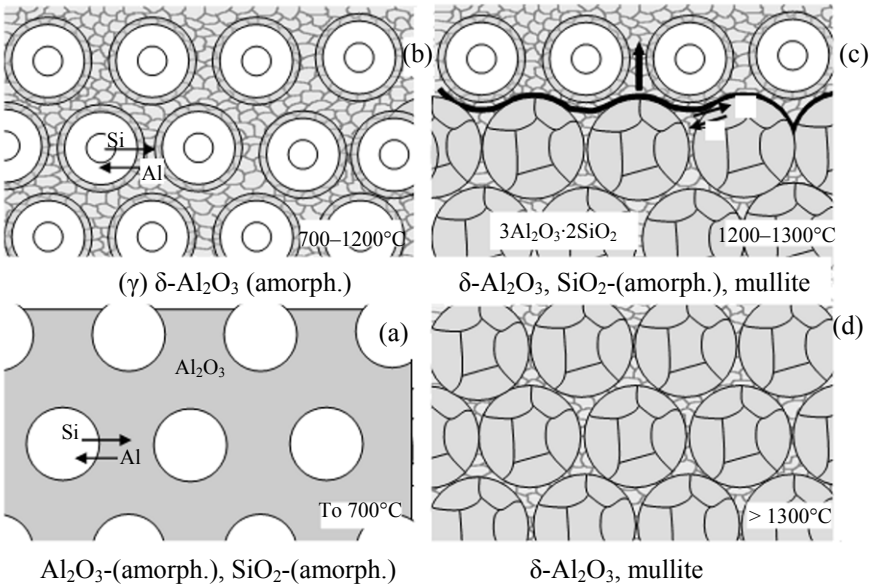

Fig. 3. Mechanism of structure formation in fibers.

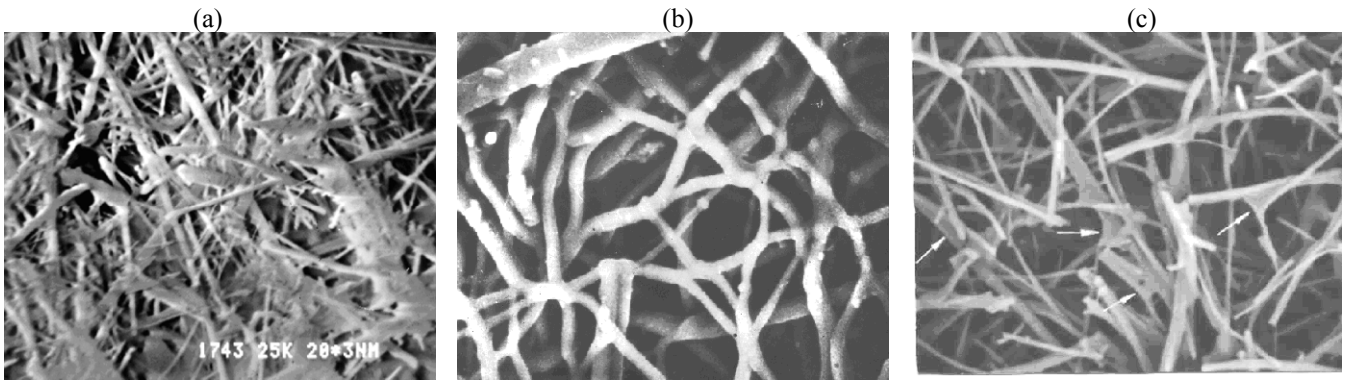

Fig. 4. Microstructure of fibrous heat shield materials (×1200): (a) VTNK, (b) TZMK-10, and (c) TZMK-1700 (SEM).

(magnification ×200000) is quite important for understanding the mechanism of formation of a stable structure. At 1250°C, extinction contours were revealed on the surface of an amorphous SiO_2 particle directly contacting with Al_2O_3. The appearance of these contours can be explained in terms of formation of mullite as a thin crystalline shell as a result of solid-phase reaction between Al_2O_3 and SiO_2. The initiation of mullite formation is also evidenced by X-ray phase analysis and data of Wei and Halloran [15]. These authors showed that mullite formation is preceded by an incubation period, a time needed for Al–Si interdiffusion and a new phase nucleation. We also observed an incubation period when prepared polycrystalline Al_2O_3 fibers by the sol–gel method.

In view of the aforesaid, we can state that the most favorable technique to form a stable structure consists in forming a 3D matrix of mullite grains (Fig. 3). To assess the probability of its formation, we performed calculations described in [14].

Taking into account that the filling degree of a dense ball packing is 74 vol %, the most appropriate composition to form the mullite matrix is 80/20 (20 wt % SiO_2), and the rest volume (26%) is occupied by an excess Al_2O_3 phase (Table 2).

In the case of a stoichiometric mullite composition, pores will initially occupy 26 vol %. If the SiO_2 content is less than 20%, the mullite matrix will not form. Thermal treatment was performed with account for the obtained results. The linear shrinkages and dispersion strengths of fibers after such thermal treatment are presented in Table 3. As seen from the table, the most thermally stable fibers contain 20 wt %

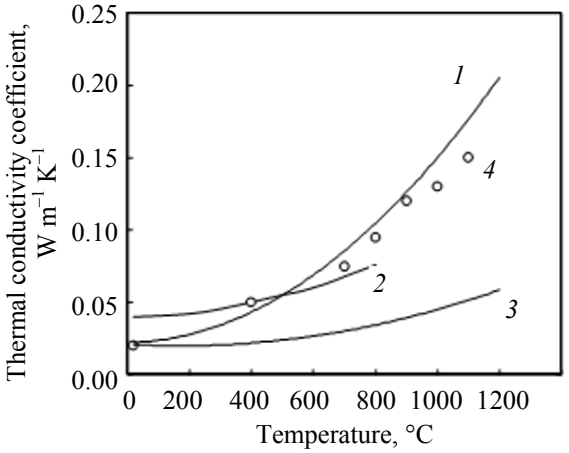

Fig. 5. Temperature dependences of the thermal conductivity of heat shield materials in a vacuum (P = 10^{-3} mm Hg): (*1*) quartz material at the Buran shuttle (g = 0.15); whisker materials: (*2*) SiC (g = 0.35); (*3*) Si_3N_4 (g = 0.15) ; and (*4*) American analog Li-900.

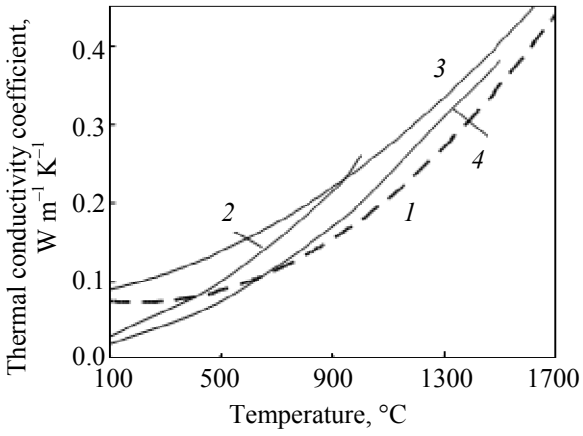

Fig. 6. Temperature dependences of fibrous materials: (*1*) TZMK-1700 (g = 0.25); foreign analogs: (*2*) Fiberfrax (g = 0.128); (*3*) Saffil (g = 0.2); and (*4*) Denka Alken (g = 0.18).

Table 4. Principal characteristics of heat shield materials on the basis of silicon nitride whiskers and quartz and alumina fibers

Characteristic	Material brand			
	VTNK	TZMK-10/2.5	TZMK-25	TZMK-1700
Density, g cm^{-3}	0.15	0.15	0.25	0.25
Working temperature, °C	1600	1250	1250	1700
Tensile strenght, MPa	0.20	0.25	0.40	0.30
LTEC, 10^{-6} deg^{-1}	2.5–3.0	0.55	0.55	6.0–9.0
Thermal conductivity, W m^{-1} K^{-1}				
20°C, 10^5 Pa	0.06	≤0.05	≤0.05	0.07
800°C, 10^5 Pa	0.16	–	–	0.13
1700°C, 10^5 Pa	–	–	–	0.42
Linear shrinkage, %				
1250°C, 36 h	0	14	14	0
1600°C, 24 h	3	–	–	2

SiO_2. It was found that the Al_2O_3 and mullite grain sizes are 5–15 and 20–50 nm, respectively.

The largest linear shrinkage (20%) at 1700°C was found in mullite fibers, which is probably explained by the destruction of the matrix comprising mullite grains and intergrain pores (as mentioned above, ~ 26 vol %), due to recrystallization of mullite grains. In differently composed fibers, the space between ball-like mullite grains is filled with the stabilizing phase δ(α)-Al_2O_3; therefore, mullite grains can grow to a limited degree, and the shrinkage is smaller. In the absence of the 3D mullite matrix (SiO_2 content below 20%), Al_2O_3 grain growth on recrystallization is limited the lower the lower SiO_2 content in the fiber. This leads to a more profound structural rearrangement, larger shrinkage, and, as a consequence, lower strength of fibers, compared with the 80/20 fibers.

The research results allowed us to suggest a mechanism of the formation of a stabilized structure of Al_2O_3/SiO_2 fibers, including formation of a 3D mullite matrix stabilized by Al_2O_3 grains which, in their turn, are stabilized by the above-mentioned mullite phase. The principal characteristics of the fibers are listed in Table 1. The drawbacks of these fibers relate to the presence in them of nonfibrous inclusions, as well as a high thermal expansion coefficient.

Quartz Fibers

The main focus of the research was put on quartz fibers, since the material on their basis seemed to hold the greatest promise in view of a combination of thermophysical and mechanical properties.

In Russia, heat shield plate materials was developed on the basis of a highly thermostable superthin quartz fiber specially created with the participation of the author at the All-Union Research Institute of Glass Plastics and Glass Fiber (Fig. 2d) and fabricated from the melt of gangue quartz [16]. Materials from this fiber, analogs of Li-900 (without a glass-forming dopant), had after 36 h at 1250°C a linear shrinkage of no more than 2–3%, and high-strengths versions (1.5% B_2O_3), generally 6–8%. Thus, it was decided to use in the construction of Buran a purely quartz material, not adding higher melting fibers, which would complicate the technology, deteriorate economic parameters, etc.

Figure 4b shows a typical microstructure of the quartz material we developed together with the Tekhnologiya Obninsk Research and Production Association [16]. At the same picture we show the structures of the heat shield material on the basis of Si_3N_4 whiskers (Fig. 4a) and Al_2O_3 fibers (Fig. 4c). Such structures are characteristic of a high degree of

fusion into a rigid carcass and are realized at various compositions and ways of introduction of fusing agents. Particular attention should be focused on the structure of the material on the basis of quartz fibers.

Heat shield materials on the basis of Al_2O_3, SiC, and Si_3N_4 fibers were developed at the RIAM, but they did not found application as a plate material, even though they were used in the Buran shuttle as other-purpose functional materials [2]. The principal characteristics of heat shield materials on the basis of quartz and Al_2O_3 fibers and Si_3N_4 and SiC whiskers are given in Table 4 and Figs. 5 and 6. Figure 5 compares the thermal conductivities at $P = 10^{-3}$ mm Hg of these materials and their American analogs.

As seen from Fig. 5, Russian materials have slightly worse parameters in a vacuum at high temperatures. This is associated with a slightly larger fiber diameter in domestic materials. At atmospheric pressure and 10 mm Hg, the thermal conductivities of domestic materials compare with those of foreign analogs. As mentioned above, silicon carbide and nitride are prone to oxidation. Naturally, the material on the basis of alumina is free of this disadvantage (Fig. 6), but its application range is limited by a high thermal expansion coefficient and, consequently, lower thermal stability, especially in comparison with quartz fibers. However, preliminary calculation at the Central Air Hydrodynamic Institute that this materials could withstand thermal loads characteristic of the wing edges and nose cone of the Buran shuttle (Table 4).

It should be noted that our developed material on the basis on alumina fibers (TZMK-1700) possesses appreciably lower thermal conductivity than known analogs. This is seen from the data in Fig. 6. We suggest that the reduced thermal conductivity is associated with a smaller fiber diameter (about 1 μm).

REFERENCES

1. *Mnogorazovyi orbital'nyi korabl' "Buran"* (Buran Space Shuttle), Semenov, Yu. P. and Lozino-Lozinskii, G.E., Eds., Moscow: Mashinostroenie, 1995.
2. Gofin, M.Ya., *Zharostoikie konstruktsii mnogorazovykh aerokosmicheskikh apparatov* (Heat-Resistant Constructions of Aerospace Shuttles), Moscow: TF "Mir" ZAO, 2003.
3. Afanas'ev, I. and Listov, I., *Novosti Kosmonavtiki*, 2003, no. 9, p. 248.
4. US Patent 3.952.083, Filed Dec. 26.1973, Appl. 427.775.
5. Leiser, D.B., Smith, M., Stewart, D.A., and Goldstein, H.E., *Ceram. Eng. Sci. Proco*., 1983, nos. 7–8, p. 551; Sears, G.W., *Acta. Met*., 1953, vol. 1, p. 457.
6. McCormick, M.J., *Adv. Ceram. Mater*., 1988, vol. 3, no. 4, p. 317.
7. Sears, G.W., *Acta. Met*., 1953, vol. 1, p. 457.
8. Wagner, R.S. and Ellis, W.C., *Appl. Phys. Lett*., 1964, vol. 4, p. 69.
9. Wagner, R.S. and Ellis, W.C., *Trans. Met. Soc. AIME*, 1965, vol. 233, p. 1053.
10. Gribkov, V.N., Silaev, V.A., Shchetanov, B.V., Umantsev, E.L., and Isaikin, A.S., *Kristallografiya*, 1971, vol. 16, no. 5, p. 982.
11. Gribkov V.N., Isaikin A.S., Portnoi K.I., Silaev V.A., and Schetanov B.V., *Kompozicionnye metallicheskie materially* (Composited Metallic Vaterials), Tumanov, A.T. and Portnogo, K.I., Eds., Moscow: ONTI, 1972, pp. 159–176.
12. Gribkov, V.N., Isaikin, A.S., Shchetanov, B.V., Umantsev, E.L., and Mukaseev, A.A., *Fiz. Khim. Obrabot. Mater*., 1973, no. 3.
13. Fridrihsberg, D.A., *Kurs kolloidnoi khimii* (Textbook on Colloid Chemistry), Leningrad: Khimiya, 1974, p. 146.
14. Shchetanov, B.V., Kablov, E.N., and Shcheglova, T.M., *Materialy 24 Mezhdunarodnoi konferentsii "Kompoziysionnye materialy v promyshlennosti"* (Proc. 24th Int. Conf. "Composite Materials in Industry," Yalta, Krym, 2004, p. 324.
15. Wei, W.-Ch. and Halloran, J.W., *J. Am. Ceram. Soc*., 1988, vol. 71, no. 7, p. 581.
16. Gribkov, V.N., Mizyurina, G.T., Shchetanov, B.V., and Lyapin, V.V., *Trudy Pervoi mezhdunarodnoi aviakosmicheskoi konferentsii "Chelovek-Zemlya-Kosmos," t. 5. Materialy i tekhnologiya proizvodstva aviakosmicheskikh system* (Proc. First Int. Aviaspace Conf. "Human–Earth–Space," vol. 1. Materials and Technology of Production of Aviaspace Systems), Moscow: Voennaya akademiya im. F.E. Dzerzhinskogo, 1995, p. 223.